

FUNDAMENTAL UNDERSTANDING OF THE DEVELOPMENT OF SCRATCH-INDUCED DAMAGES
IN POLYMERS

A Thesis

by

NIKHIL REDDY AENUGU

Submitted to the College of Graduate Studies
Texas A&M University-Kingsville
in partial fulfillment of the requirements for the degree of

MASTER OF SCIENCE

December 2018

Major Subject: Mechanical Engineering

ProQuest Number:22624171

All rights reserved

INFORMATION TO ALL USERS

The quality of this reproduction is dependent on the quality of the copy submitted.

In the unlikely event that the author did not send a complete manuscript and there are missing pages, these will be noted. Also, if material had to be removed, a note will indicate the deletion.



ProQuest 22624171

Published by ProQuest LLC (2019). Copyright of the Dissertation is held by the Author.

All Rights Reserved.

This work is protected against unauthorized copying under Title 17, United States Code
Microform Edition © ProQuest LLC.

ProQuest LLC
789 East Eisenhower Parkway
P.O. Box 1346
Ann Arbor, MI 48106 - 1346

FUNDAMENTAL UNDERSTANDING OF THE DEVELOPMENT OF SCRATCH-INDUCED
DAMAGES IN POLYMERS

A Thesis

by

NIKHIL REDDY AENUGU

Approved as to style and content by:



Mohammad Motaher Hossain, Ph.D.
(Chair of Committee)



Shah Alam, Ph.D., P.E.
(Member of Committee)



Dervis Emre Demirocak, Ph.D.
(Member of Committee)



Larry Peel, Ph.D., P.E.
(Chair of Department)



George Allen Rasmussen, Ph.D.
(Vice President for Research and Graduate
Studies)

December 2018

ABSTRACT

Fundamental Understanding of the Development of Scratch-induced Damages in Polymers

(December 2018)

Nikhil Reddy Aenugu, B.E., Manipal University, India

Chairman of Advisory Committee: Dr. Mohammad Motaher Hossain

Scratch performance of polymers is very important considering its wide range of applications in optical, automotive, electrical and household appliances where long term wear and tear of material is critical. The objective of this research is to study the scratch-induced damage in polymers using experimental study on model polymers and finite element method (FEM) modeling. Uniaxial tensile testing and scratch testing with variation in speed are carried out on acrylic and polycarbonate (PC) and the results are analyzed and discussed. Efforts are made to relate rate dependent mechanical behavior with the scratch behavior of polymers. Three-dimensional finite element method (FEM) modeling has also been carried out to simulate the crack formation during the scratching process. Effects of material and surface properties on scratch-induced damages in polymers have been investigated. The study provided useful insights on designing scratch resistant polymers.

ACKNOWLEDGEMENTS

I would like to express great appreciation to Dr. Mohammad Motaher Hossain for his valuable and constructive suggestions throughout the conception and development of my thesis work. His generosity with his time has been held in the highest of regard.

My sincere thanks to Dr. Shah Alam and Dr. Dervis Emre Demirocak, my committee members for their guidance and extensive help in supporting my thesis.

I would like to thank the entire faculty of the Department of Mechanical Engineering for their support and for blessing me with enormous knowledge through my coursework in this university.

I would also like to thank Mr. Carlos Hinojosa for his technical assistance in sample preparation for uniaxial tensile testing.

Finally, I would also like to thank my parents, my friends, and all my family members for their constant encouragement and inspiration that kept me charged and confident while pursuing my master's degree and throughout my life, without whom it would have never been possible.

TABLE OF CONTENTS	Page
ABSTRACT.....	iii
ACKNOWLEDGEMENTS.....	iv
TABLE OF CONTENTS.....	v
LIST OF FIGURES.....	vii
LIST OF TABLES.....	ix
CHAPTER I INTRODUCTION.....	1
1.1 Scratch.....	1
1.2 Objectives of the Research.....	4
CHAPTER II LITERATURE REVIEW.....	5
2.1 Effect of Surface Friction and Material Properties on Scratch Behavior.....	7
CHAPTER III EXPERIMENTAL WORK.....	11
3.1 Materials.....	11
3.2 Sample Preparation and Tensile Testing.....	11
3.2.1 Results and Discussion.....	13
3.3 Scratch Testing and Analysis.....	20
CHAPTER IV FEM MODELING AND ANALYSIS.....	27
4.1 Effect of Ductility on Onset of Cracking.....	29
4.2 Effect of Strength on Onset of Cracking.....	31
4.3 Effect of Coefficient of Surface Friction on Onset of Cracking.....	33
4.4 Effect of Material Stiffness on Onset of Cracking.....	37
CHAPTER V CONCLUSION AND FUTURE SCOPE.....	39

5.1 Conclusions.....	39
5.2 Future Work.....	41
REFERENCES.....	42
VITA.....	45

LIST OF FIGURES	Page
Figure 1. Evolution map of scratch damage.....	2
Figure 2. Different types of scratch-induced damages in polymers.....	3
Figure 3. Different steps in scratching process.....	5
Figure 4. Scratch depth vs. scratch length.....	8
Figure 5. Scratch depth vs. Poisson's ratio.....	8
Figure 6. Evolution of scratch.....	9
Figure 7. Crack formation during scratching.....	9
Figure 8. Schematic of a tensile sample used in this study.....	12
Figure 9. MTS criterion model 45 tensile testing machine.....	13
Figure 10. Yield stress of PC at different crosshead speeds.....	15
Figure 11. Fracture strain of PC at different crosshead speeds.....	15
Figure 12. Young's modulus of PC at different crosshead speeds.....	16
Figure 13. Rate dependent stress-strain response of PC	16
Figure 14. Fracture stress of acrylic at different crosshead speeds.....	18
Figure 15. Fracture strain of acrylic at different crosshead speeds	19
Figure 16. Young's modulus of acrylic at different crosshead speeds.....	19
Figure 17. Rate dependent stress-strain response of acrylic.....	20
Figure 18. Scratch machine used for testing.....	21
Figure 19. Onset of cracking in acrylic at 1 mm/s.....	22
Figure 20. Onset of cracking in acrylic at 10 mm/s	22
Figure 21. Onset of cracking in acrylic at 100 mm/s	23
Figure 22. Onset load for cracking of acrylic at different scratch speeds.....	23

Figure 23. Images of scratch width along the scratch length for PC.....	24
Figure 24. Scratch width as a function of scratch length for PC.....	26
Figure 25. FEM model with a spherical tip of 1 mm diameter.....	27
Figure 26. Typical material response showing progressive damage.....	28
Figure 27. Maximum principle stress contour of materials with different ductility.....	31
Figure 28. Maximum principle stress contour for materials with different strengths	33
Figure 29. Maximum principle stress contour for FEM models with different coefficient of friction (COF).....	35
Figure 30. Maximum principle stress contour for FEM models at a load of 5.8 N.....	36
Figure 31. Maximum principle stress contour for FEM models at a load of 25.1 N.....	36
Figure 32. Maximum principle stress contour for FEM models with different Young's modulus.....	38

	Page
LIST OF TABLES	
Table 1. PC properties of three different samples for a crosshead speed of 0.5 mm/min.....	14
Table 2. PC properties of three different samples for a crosshead speed of 5 mm/min.....	14
Table 3. PC properties of three different samples for a crosshead speed of 50 mm/min.....	14
Table 4. Acrylic properties of three different samples for a crosshead speed of 0.5 mm/min.....	17
Table 5. Acrylic properties of three different samples for a crosshead speed of 5 mm/min.....	17
Table 6. Acrylic properties of three different samples for a crosshead speed of 50 mm/min.....	18
Table 7. Onset load for cracking of acrylic at different scratch speed.....	23
Table 8. Scratch widths of PC for four different scratches at 1 mm/s for different scratch lengths.....	25
Table 9. Scratch widths of four different scratches at 10 mm/s for different scratch lengths.....	25
Table 10. Scratch widths of four different scratches at 100 mm/s for different scratch lengths.....	25
Table 11. Triaxiality data used for the FEM modeling.....	29
Table 12. Material properties used for FEM modeling to study the effect of ductility.....	30
Table 13. Material properties used for FEM modeling to study the effect of strength.....	32
Table 14. Material properties used for FEM modeling to study the effect of COF.....	34
Table 15. Material properties used for FEM modeling to study the effect of stiffness.....	37

CHAPTER I

INTRODUCTION

1.1 Scratch

The scratching process is defined as the material deformation when a force is applied on the surface of a material with a rigid tip [1]. Scratch behavior of polymers has received significant attention in the recent past as surface quality of polymers in electronic, optical, structural, and automotive applications are becoming more and more important. For instance, in the interior and exterior parts of an automotive, scratches and noticeable surface damages are undesired because it can reduce the product value significantly. Polymers are more vulnerable to surface damage when compared to metals and ceramics [2]. Compared to metals, the behavior of polymers is very different due to the viscoelastic and viscoplastic nature of polymers. Establishing relationship between different material properties, surface properties and scratch damage features could facilitate understanding the scratch-induced damage mechanisms and their evolution processes. Scratch behavior is affected by several parameters such as coefficient of friction, applied load, scratch speed, viscoelastic recovery, material properties, geometry of the tip, etc. [3].

Two different types of scratch damage generally observed in polymers, i.e., ductile damage and brittle damage, depending on the material types and applied load [2]. Understanding the surface damage evolution process in polymers with increasing normal loads and corresponding stress values are critical to establish a relationship between material parameters and scratch behavior. The typical surface damage mechanisms in scratching process can be classified as groove

formation, micro plowing, micro cutting, and microcracking. Scratch damages on polymer surface depends on the severity of applied load and the types of material involved. Figure 1, shows the schematics of different types of scratch damages that formed during the increasing normal load scratching process, following the ASTM scratch testing standard. The different scratch zones are initial surface damage zone (mar), followed by cracking/fish-scale zone (depending on the material type), which is followed by material removal with increase in normal load.

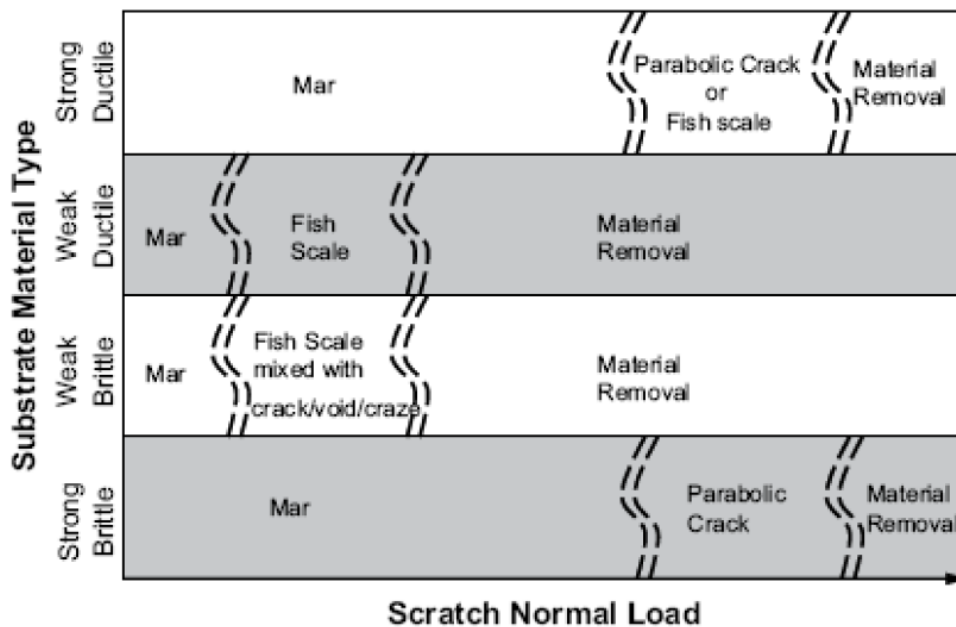


Figure 1. Evolution map of scratch damage [2].

Initial damage zone is where the tip meets the substrate and there is only a minor surface deformation is observed. This includes non-recoverable plastic deformation; time dependent viscoelastic deformation and fully recoverable elastic deformation due to compression of material in front of the tip, called mar damage. With further increase in normal load, material can

undergo large plastic deformation and form fish-scales shown in Figure 2(a), or cracks shown in Figure 2(b), depending on material types and loading conditions. Finally, material removal shown in Figure 2(c), will occur as the load continues to increase and tip penetrates through the surface [1].

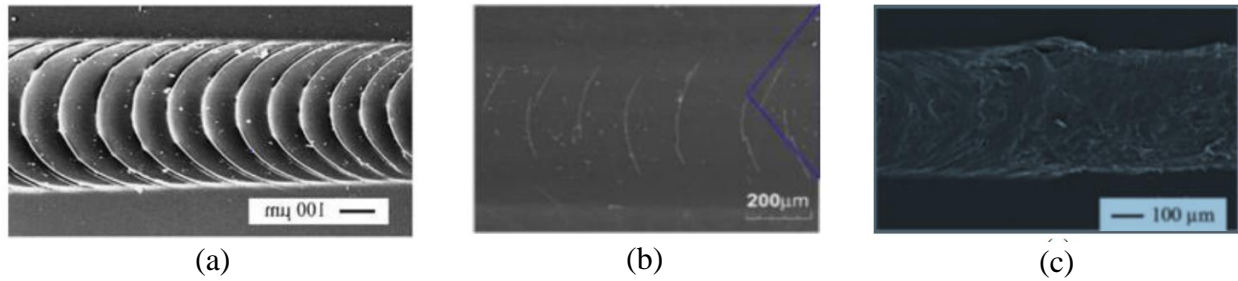


Figure 2. Different types of scratch-induced damages in polymers (a) Fish-scale; (b) Parabolic crack; (c) Material removal [2].

Researchers have used finite element method (FEM) modeling as the numerical technique to study the scratch mechanics due to its capability to handle complicated aspects of scratch problem. The primary objective of performing FEM modeling on scratching is to investigate the response of material surface under the application of a normal load as well as the damage mechanisms involved. A three-dimensional FEM parametric study is important to establish relationship between material and surface properties with scratch damage mechanisms, which can facilitate understanding the scratch damages in polymers. FEM can also help simulating certain scratch damage features, such as crack formation to study the complex stress state involved in the crack formation. All these will enable understanding the scratch mechanics as well as developing scratch resistant polymers for various applications.

1.2 Objectives of the Research

The goal of the study is to understand the scratch-induced surface damages in polymers using FEM modeling and experimental study. Relationship between rate dependent mechanical behavior and scratch behavior is sought in this study to establish relationship between material properties and surface damages due to scratching. As mentioned, FEM modeling can help understanding the scratch mechanics, and establishing the above-mentioned relationship. FEM modeling has been carried out to study crack formation during scratching, a surface damage feature generally observed in brittle polymers. Crack formation during scratching can cause a structure to fail prematurely. Therefore, understanding the origin and evolution of crack formation during scratching is very important. FEM analysis and experimental work were carried out to study how material and surface properties influence crack formation during scratching.

The specific objectives (deliverables) are to:

1. Develop FEM models to simulate scratch-induced damages, specifically crack formation in polymers.
2. Analyze the underlying mechanics associated with the surface damage features.
3. Study the effects of various material and surface properties on crack formation during scratching in polymers.
4. Validate FEM findings using experimental observation on polymers.
5. Relate rate dependent mechanical behavior with the scratch behavior in polymers.

All the above-mentioned objectives are achieved.

CHAPTER II

LITREATURE REVIEW

Maintaining surface quality in the long run is often the most important attribute for optimal functionality of a product. The polymers used in automotive interiors and exteriors are extremely prone to scratching which will degrade the appearance [7]. Researchers over the years tried to link certain surface damage features and transitions with material properties to provide guidelines to produce surface damage resistant polymers.

Figure 3, represents the steps in the scratching process according to the ASTM standard; the first step is the indentation step Figure 3(a), where the scratch tip (generally 1 mm diameter) indents the surface of the polymer substrate with a prescribed normal load. The second step is the scratching step Figure 3(b), where the tip scratches along the length of the surface of substrate with a specified normal load and speed, and finally, the scratch tip is lifted from the surface of the substrate by moving it vertically upward Figure 3(c).

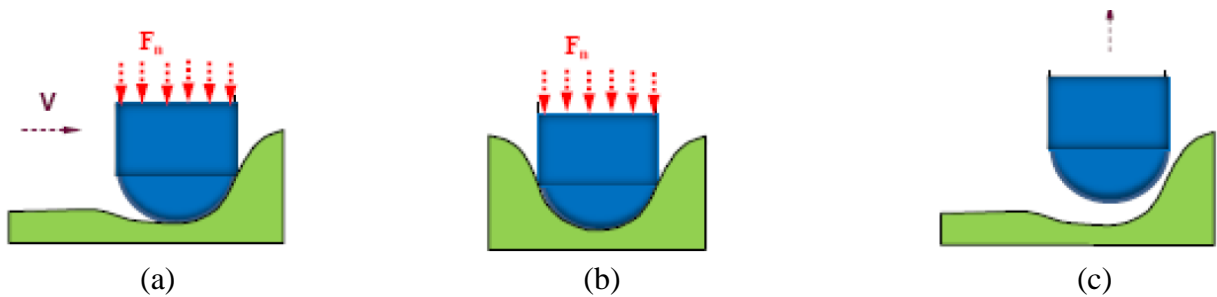


Figure 3. Different steps in scratching process (a) Indentation of tip on the surface; (b) Scratching the surface with the tip; (c) Removing the tip from the surface after the scratching [8].

The speed or rate of loading is very important in determining how the material is performing in a particular scenario. As the loading speed increases, the material is being loaded at a faster rate and this tends to generally increase the strength and stiffness of materials, although the material behaves in more brittle fashion. Since mechanical behavior of polymers shows significant rate dependence, scratch behavior of polymers can also be dependent on the scratching speed. As the scratch speed increases, surface damages in polymers can have a ductile to brittle transition. The polymers that show significant ductility at lower speed can have crack formation during high speed scratch testing due to this transition. Other surface damage features, such as scratch groove can be influenced by the scratching speed, as well.

Finite Element Method (FEM) modeling is an important tool in understanding the mechanics because it can show the complex stress state and deformation of the entire structure whereas the experiments cannot. Moreover, various parameters can be changed at ease when modeling such as density, Young's modulus, strength etc. by which time and effort in conducting test on actual material can be saved. FEM can explain the mechanics of surface damages during scratching such as crack formation, and how crack formation varies with change in material and surface parameters. Material behavior can affect the crack formation during scratching. Different polymer types such as ductile or brittle polymers shows different type of crack formation. Crack formation during scratching has significant impact on product value from aesthetic point of view. It can also act as the starting point for structural failure.

2.1 Effect of Surface Friction and Material Properties on Scratch Behavior

Surface friction is a crucial factor which influences scratch-induced damages. Stress state of the polymer surface changes with varying surface friction. It is very important to know how exactly surface friction affects the scratch induced deformation, so through FEM analysis, the scratch behavior due to change in friction can be studied, and one can minimize its effect on the scratch deformation [9]. Using elastic-perfectly-plastic model in FEM, it was observed that the scratch depth increases with increasing COF with all other parameters kept the same [9]. Two critical parameters that affect scratch depth according to the study were COF and yield stress [9]. Hossain et al. performed FEM analysis where the strain softening-strain hardening phenomenon was considered [10]. The simulation showed that yield stress and strain at stress recovery are the most crucial factors that influence the scratch depth. Higher strain hardening slope induces shallower scratch depth if all other parameters are kept constant. Also, increase in strain at stress recovery induces deeper scratch depth and higher shoulder height [11]. Moreover, with the reduction of COF it was observed that the scratch resistance increases [12]. Increasing the yield stress induces lower scratch depth Figure 4(a), whereas stiffer strain softening slope induces deeper scratch depth Figure 4(b), in scratched materials [12]. Poisson's ratio has no effect on scratch behavior, as shown in Figure 5 [11].

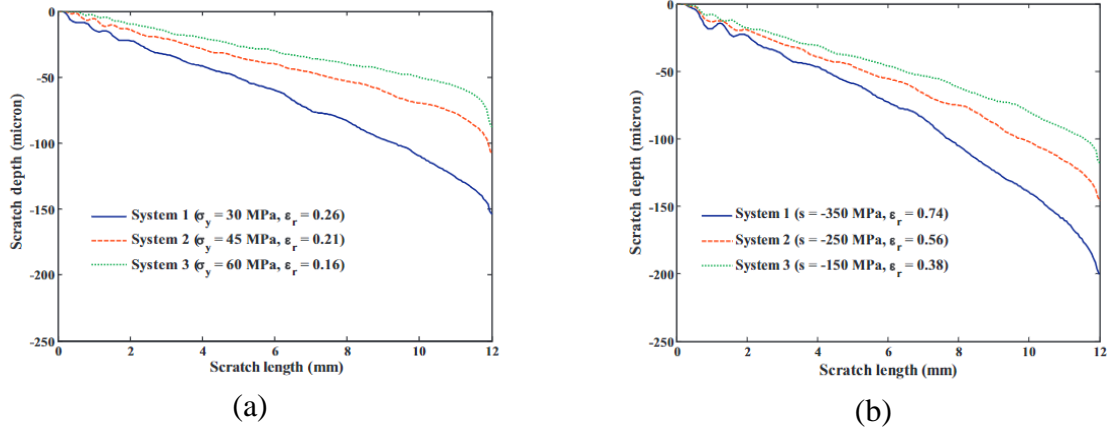


Figure 4. Scratch depth vs. scratch length (a) Effect of yield stress on scratch depth; (b) Effect of strain softening slope on scratch depth [12].

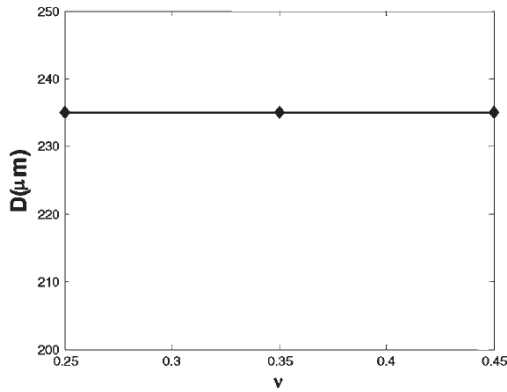


Figure 5. Scratch depth vs. Poisson's ratio [11].

There are different damage zones observed during scratching such as the initial damage zone, cracking/crazing/fish-scale zone and material removal zone. The initial damage zone is where the tip indents the surface of the polymer substrate. Then as the tip progresses along the surface of the polymer substrate, small amount of deformation is observed along the scratch path under a low load and stress level. With the increase in load there will be periodic damage pattern in the scratch direction due to plastic deformation or crack formation. This change from the initial damage zone to the cracking/crazing/fish-scale zone is due to the increase in load. The fish scale

damage is one of the most dominant types of surface damage observed in polymers due to drawing of material under the tip surface [2]. The change from the initial damage zone to cracking/crazing/fish-scale zone in this case is shown in Figure 6(a), and Figure 6(b), represents a fully developed fish-scale formation. As the load increases the scratch tip goes through the surface of the polymer substrate causing material removal from the surface. This change from the formation of fish-scale to the plowing of the material is shown in Figure 6(c). This repeated surface damage features generally observed in highly ductile polymers.

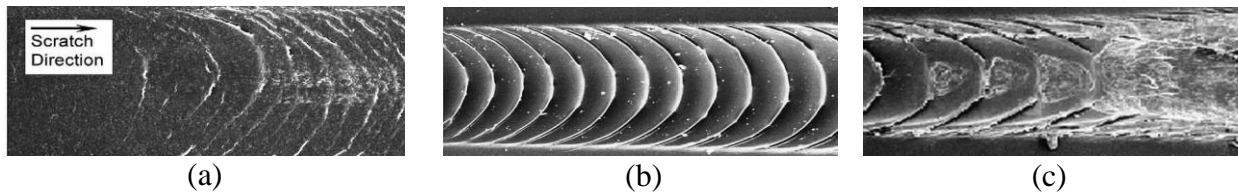


Figure 6. Evolution of scratch (a) Transition from initial damage zone to scratch zone; (b) Fully developed fish scale formation; (c) Change from fish scale to material removal [2].

As the scratch tip moves along the surface of the substrate with increasing normal load the material under the scratch tip and the material in front of the scratch tip undergoes very complex stress state with the stresses change from compressive to tensile [13]. When a high normal load is applied on brittle polymers, parabolic crack tends to form on the scratch path as shown in Figure 7(a). This kind of periodic damage which generally forms perpendicular to the scratch direction is a typical brittle surface damage feature [14]. Figure 7(b), represents the change in scratch behavior from mar damage to parabolic crack zone and once the load reaches a critical value, the change from parabolic crack to material removal takes place as shown in Figure 7(c).

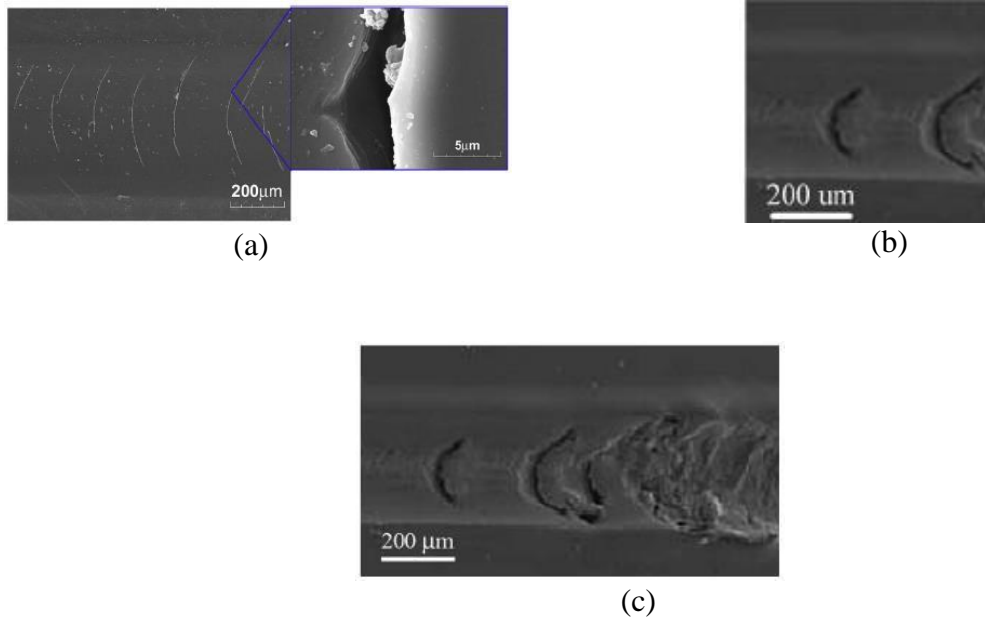


Figure 7. Crack formation during scratching (a) In epoxy; (b) In PC; (c) Change from parabolic crack to material removal in PC [2].

There has not been any significant research on the simulation of crack formation in polymers during scratching, although this research would help understanding the scratch behavior of brittle polymers and will aid in designing scratch resistant polymers. It is also important to know how the material properties affect the scratch-induced damages in polymers.

CHAPTER III

EXPERIMENTAL WORK

This chapter discusses about the materials used, samples prepared, and tests conducted on two different polymers. Uniaxial tensile testing with different crosshead speeds and scratch testing were carried out, and the results are analyzed and discussed.

3.1 Materials

One ductile polymer and a brittle polymer were chosen in this research to understand the scratch behavior of both ductile and brittle polymers. The materials used for the experiments are Makrolon GP Polycarbonate (PC) sheets from A&C Plastics Inc. and Acrylic sheets from Interstate Plastics. This specific type of PC has high impact resistance. PC is extensively used in glazing and industrial applications. Acrylic is a lightweight alternative to glass. Its excellent optical properties and impact resistance make it an ideal replacement for glass in rough weather conditions where glass may shatter.

3.2 Sample Preparation and Tensile Testing

To prepare samples for tensile testing, polymer sheets were cut to the approximate rectangular sizes to fit in the dog bone shaped specimens after machining. The specimens were machined using a vertical milling machine. A clamp was made to hold the specimen on the bed since the specimen alone could not be placed on the bed because of the thickness of the material. Afterwards, the samples were polished on the edges to eliminate any irregularities which may act as a stress concentration zone. Figure 8, shows the schematic of the tensile samples used in this

study along with the dimension, prepared according to the ASTM D638 Type IV standard [15]. All the samples were 3 mm in thickness.

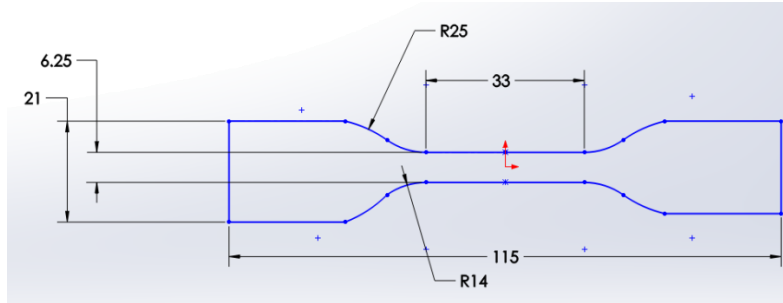


Figure 8. Schematic of the tensile sample used in this study (all dimensions are in “mm”).

Uniaxial tensile testing was carried out following the ASTM D638 standard [15]. A screw driven MTS machine equipped with a load cell of 100 KN was used for all the tensile tests. MTS TWE Elite software interface was used to collect the data from the testing. The samples were tested on the MTS criterion model 45 tensile testing machine (Figure 9) at three different crosshead speeds of 0.5 mm/min, 5 mm/min, and 50 mm/min. A minimum of three samples were tested for each crosshead speeds to obtain the average value and standard deviation.



Figure 9. MTS criterion model 45 tensile testing machine.

3.2.1 Results and Discussion

Data acquired from the tensile testing of PC are given below in Tables 1-3 for three different crosshead speeds of 0.5 mm/min, 5 mm/min and 50 mm/min, respectively. Figure 10, shows the true yield stress values obtained from the uniaxial tensile testing as a function of crosshead speed for PC. The true yield stress values were obtained from the engineering stress-strain data from the uniaxial tensile testing. It can be seen that the true yield stress increases with the increase in crosshead speed. Figure 11, shows the fracture strain as a function of crosshead speed for PC. It can be seen that the fracture strain decreases with the increase in crosshead speed. Figure 12, shows the Young's modulus as a function of crosshead speed for PC. It can be seen that there is a slight increase in Young's modulus as the crosshead speed increases. From the above experimental observations, it can be concluded that as the crosshead speed increases the PC

becomes more brittle, strong and stiff. Figure 13, shows the rate dependent stress-strain response of PC and it can be seen that the post- yielding behavior of PC in tension is almost the same.

Table 1. PC properties of three different samples for a crosshead speed of 0.5 mm/min.

0.5 mm/min	PC sample-1	PC sample-2	PC sample-3	Average	Standard deviation
Yield stress (MPa)	59.07074	59.04011	61.00919	59.70669	1.12811
Fracture strain (mm/mm)	0.550636	0.583556	0.608454	0.580882	0.029001
Young's modulus (MPa)	1160.5	1231.3	1191.6	1194.4	35.4

Table 2. PC properties of three different samples for a crosshead speed of 5 mm/min.

5 mm/min	PC sample-1	PC sample-2	PC sample-3	Average	Standard deviation
Yield stress (MPa)	61.97659	62.45490	65.70057	63.37736	2.02612
Fracture strain (mm/mm)	0.508154	0.43629	0.506915	0.483788	0.041135
Young's modulus (MPa)	1185.8	1249.2	1274.9	1236.6	45.8

Table 3. PC properties of three different samples for a crosshead speed of 50 mm/min.

50 mm/min	PC sample-1	PC sample-2	PC sample-3	Average	Standard deviation
Yield stress (MPa)	61.88607	66.64199	69.35178	65.95995	3.77929
Fracture strain (mm/mm)	0.412942	0.393370	0.345113	0.383808	0.034910
Young's modulus (MPa)	1340.0	1441.6	1280.1	1353.9	81.6

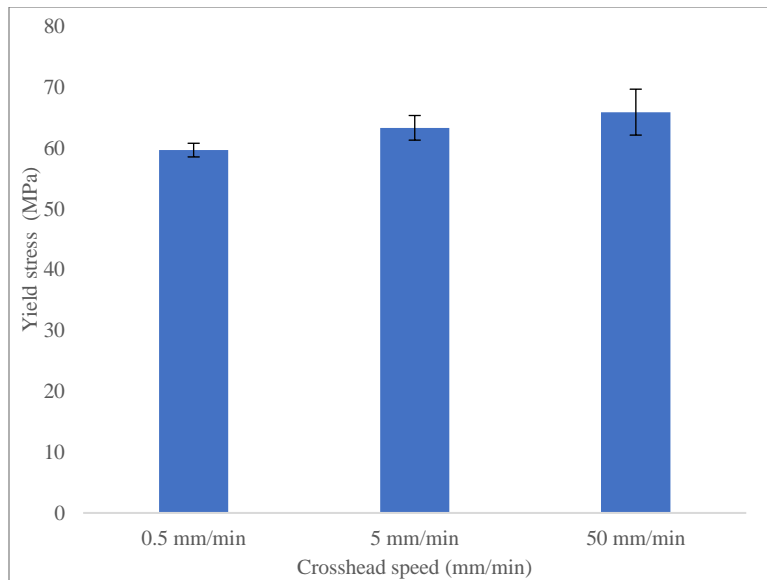


Figure 10. Yield stress of PC at different crosshead speeds.

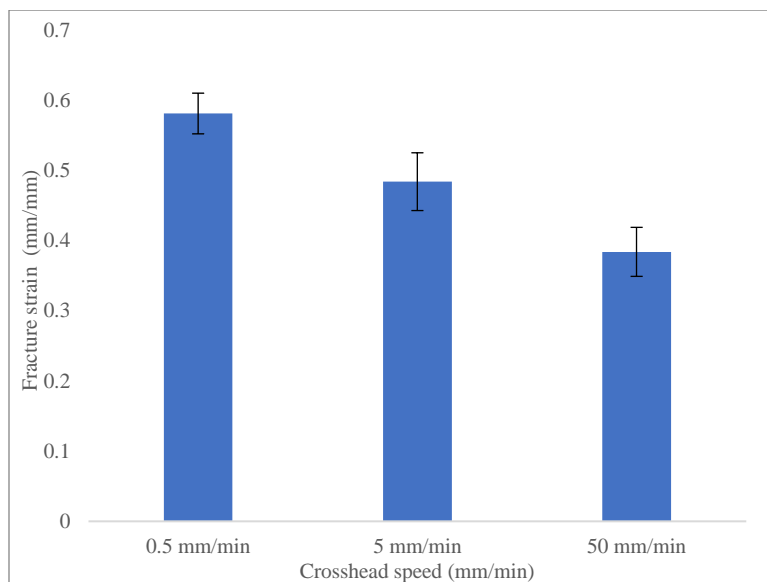


Figure 11. Fracture strain of PC at different crosshead speeds.

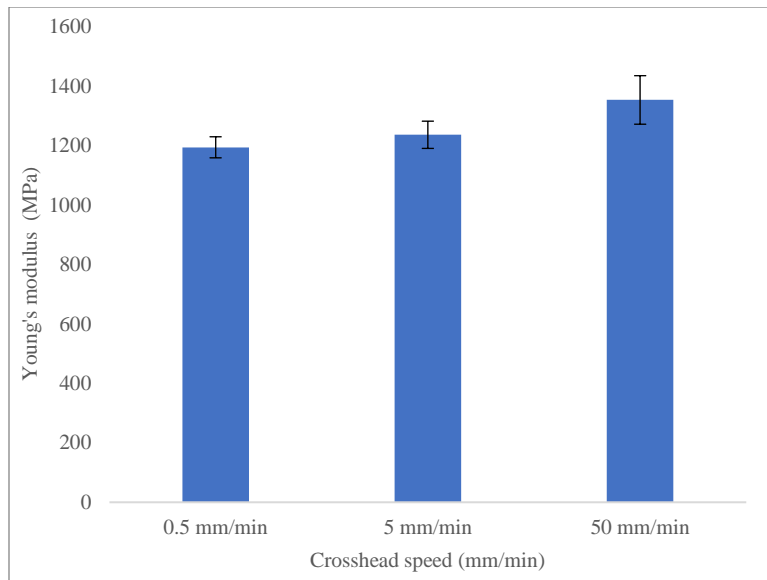


Figure 12. Young's modulus of PC at different crosshead speeds.

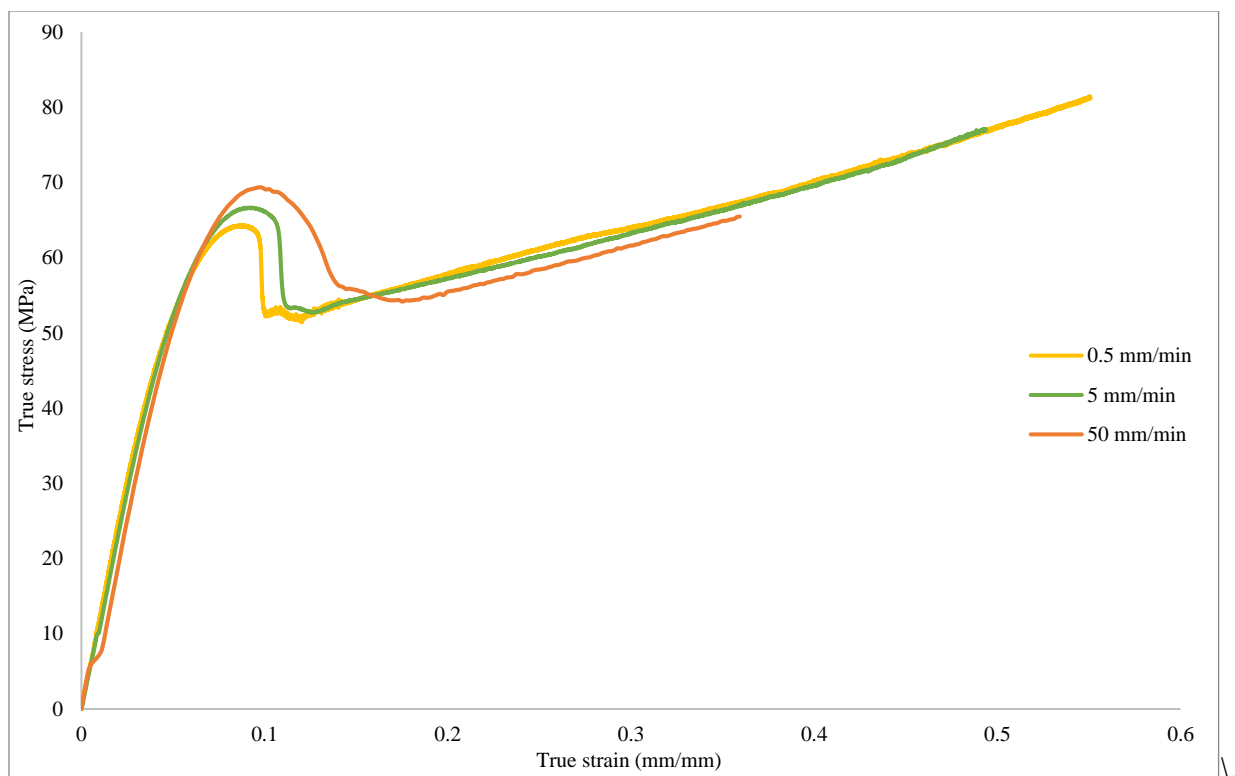


Figure 13. Rate dependent stress-strain response of PC.

Data acquired from the tensile testing of acrylic samples are shown below in Tables 4-6 for three different crosshead speeds of 0.5 mm/min, 5 mm/min and 50 mm/min, respectively. Figure 14, shows the true fracture stress values obtained from the uniaxial tensile testing as a function of crosshead speed. The true fracture stress values were obtained from the engineering stress-strain data from uniaxial tensile testing. It can be seen that the fracture stress decreases slightly with the increase in crosshead speed. Figure 15, shows the fracture strain as a function of crosshead speed. It can be seen that there is a decrease in strain to failure as crosshead speed increases. Figure 16, shows the Young's modulus as a function of crosshead speed. It can be seen that there is a slight increase in Young's modulus as the crosshead speed increases. From the above observations it can be said that as the crosshead speed increases the acrylic becomes more brittle, strong and stiff. Figure 17, shows the rate dependent stress-strain response of acrylic.

Table 4. Acrylic properties of three different samples for a crosshead speed of 0.5 mm/min.

0.5 mm/min	Acrylic sample-1	Acrylic sample-2	Acrylic sample-3	Average	Standard deviation
Fracture stress (MPa)	46.23976	54.87990	57.63268	52.91745	5.94458
Fracture strain (mm/mm)	0.119320	0.106272	0.096742	0.107445	0.011334
Young's modulus (MPa)	1444.3	1436.9	1559.7	1480.3	68.8

Table 5. Acrylic properties of three different samples for a crosshead speed of 5 mm/min.

5mm/min	Acrylic sample-1	Acrylic sample-2	Acrylic sample-3	Average	Standard deviation
Fracture stress (MPa)	73.12204	70.31267	60.61332	68.01602	6.56300
Fracture strain (mm/mm)	0.079786	0.078306	0.058214	0.072103	0.012049
Young's modulus (MPa)	1712.5	1680.4	1594.4	1662.4	61.0

Table 6. Acrylic properties of three different samples for a crosshead speed of 50 mm/min.

50mm/min	Acrylic sample-1	Acrylic sample-2	Acrylic sample-3	Average	Standard deviation
Fracture stress (MPa)	76.74154	66.20777	68.53380	70.49437	5.53380
Fracture strain (mm/mm)	0.075862	0.069579	0.069580	0.071674	0.003627
Young's modulus (MPa)	1575.4	1777.2	1672.2	1674.9	100.9

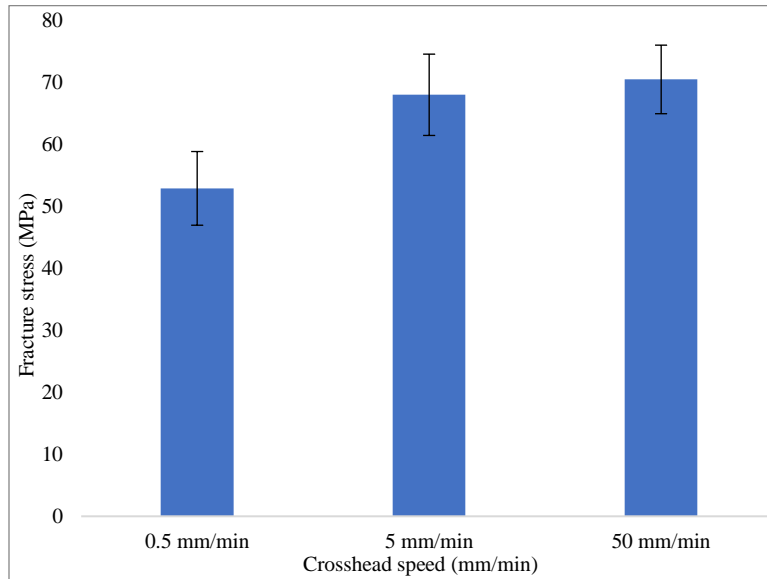


Figure 14. Fracture stress of acrylic at different crosshead speeds.

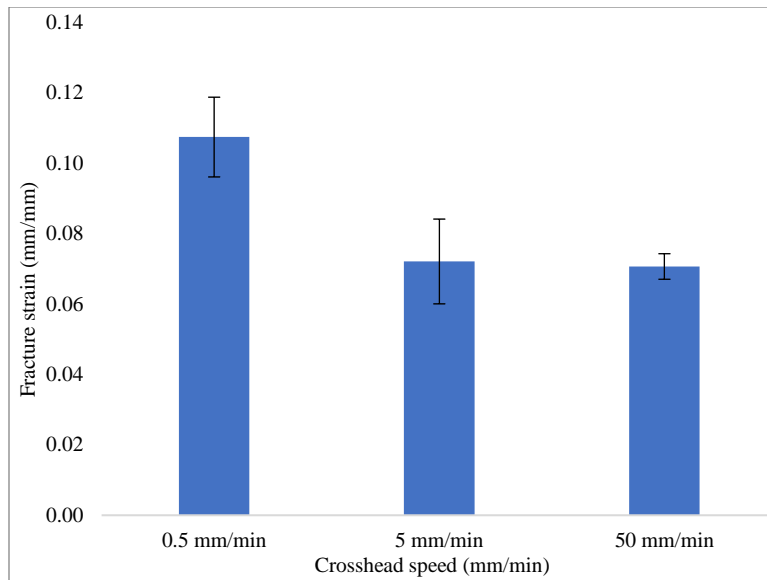


Figure 15. Fracture strain of acrylic at different crosshead speeds.

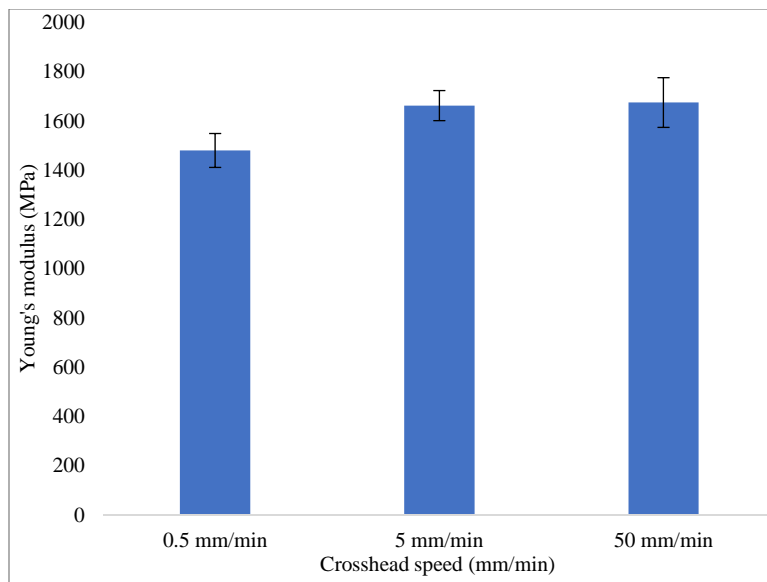


Figure 16. Young's modulus of acrylic at different crosshead speeds.

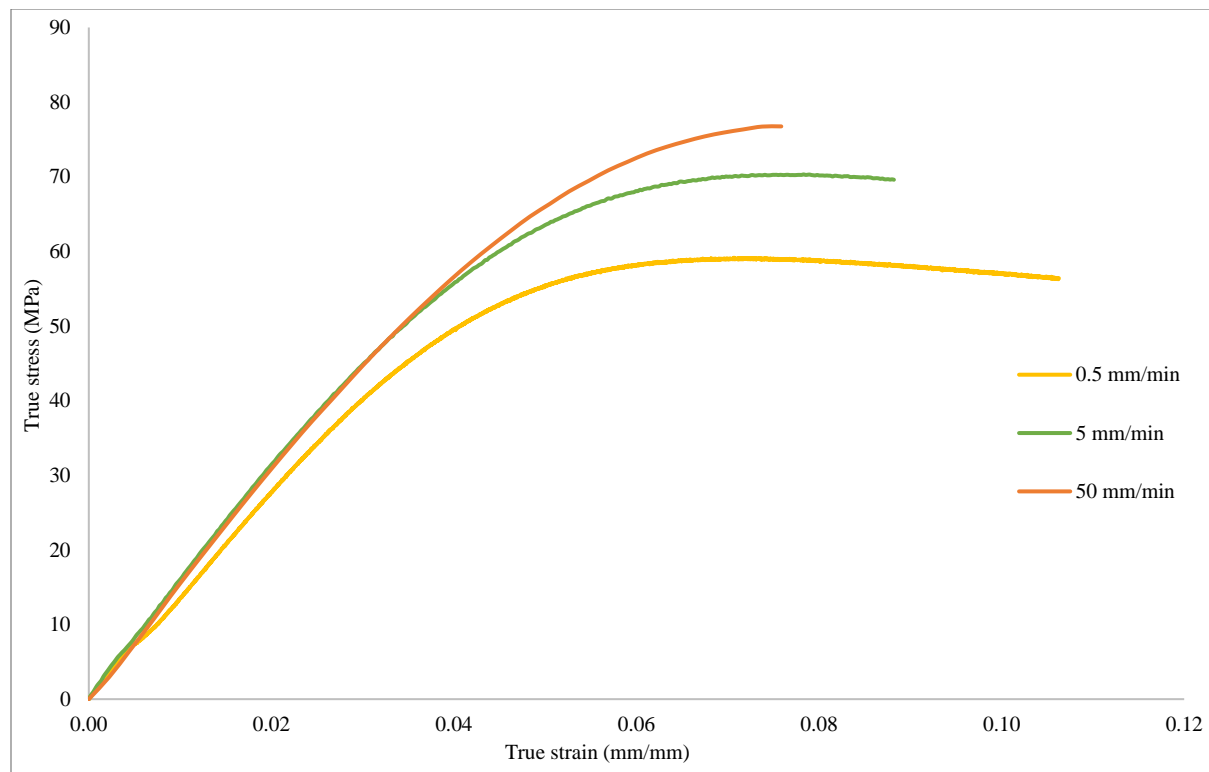


Figure 17. Rate dependent stress-strain response of acrylic.

3.3 Scratch Testing and Analysis

Scratch tests were carried out on acrylic and PC samples by employing a gradually increasing normal load of 1-90 N and 1-100 N, respectively. Three scratch speeds of 1 mm/s, 10 mm/s and 100 mm/s were used for the scratch tests with a scratch length of 100 mm. Compressed air was used during each test to clear out any dust particles present on the samples. The scratch machine used for the testing is shown in Figure 18. For the scratch testing, a tungsten carbide spherical tip with a diameter of 1 mm was used. After the scratch tests, onset of cracking was determined for acrylic, however, no crack was observed in PC at 100 N. A Nikon EPIPHOT 300 Metallurgical Microscope was used for the analysis of scratch-induced damages in polymers. Microcapture software was used to obtain the high-resolution images of the scratched surface. How the varying

scratch speed affects the scratch width along the scratch length for PC and onset of cracking for acrylic were analyzed.

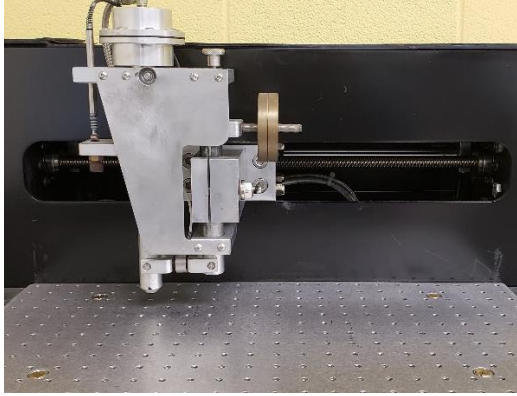


Fig. 18 Scratch machine used for testing.

For acrylic, a total of 4 scratch tests were done for each speed and the samples were examined under the microscope to find the onset of cracking. After finding the length for the onset of cracking, the load at that scratch length was obtained from the scratch test data file and this procedure was repeated for all three speeds. The average loads and standard deviation for three different scratch speeds are shown in Table 7. Figures 19-21, show the images of onsets of cracking for acrylic at scratch speeds of 1 mm/s, 10 mm/s, and 100 mm/s, respectively. The images of onset of cracking were taken with the microscope at 5X, 10X and 20X magnification. The black arrow on the images indicate the scratch direction. The cracks for acrylic look parabolic in shape. The cracking is presumably due to tensile stress behind the scratch tip caused by the tip on the material surface during the scratching process. For acrylic as the scratch speed increases, the scratch length and, therefore the load for onset of crack formation decreases, as shown in Figure 22. From the tensile testing it was observed that as the crosshead speed increases the material becomes more brittle (Figure 17). Similarly when scratch tests were

conducted on acrylic it can be seen that as the scratch speed increases, the onset load for cracking decreases, as the polymer behaves more in brittle fashion with increase in speed.

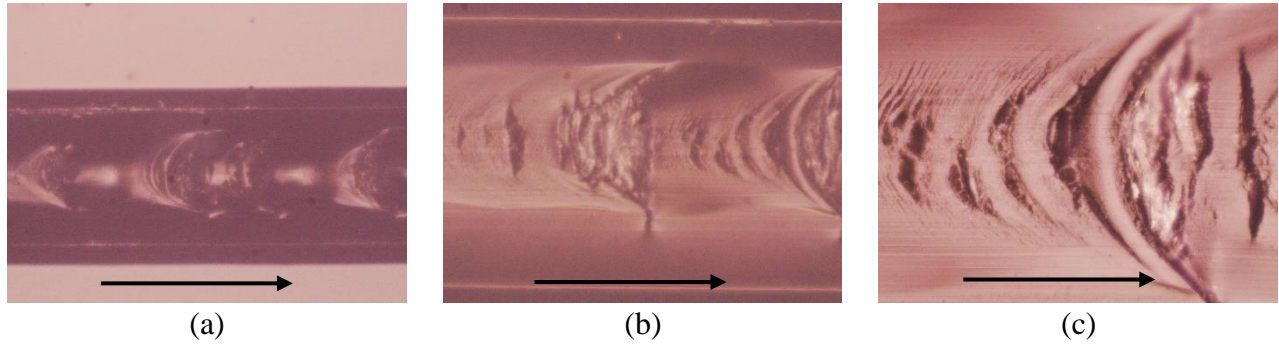


Figure 19. Onset of cracking in acrylic at 1 mm/s (a) 5X magnification; (b) 10X magnification; (c) 20X magnification. (Black arrow indicates the scratch direction)

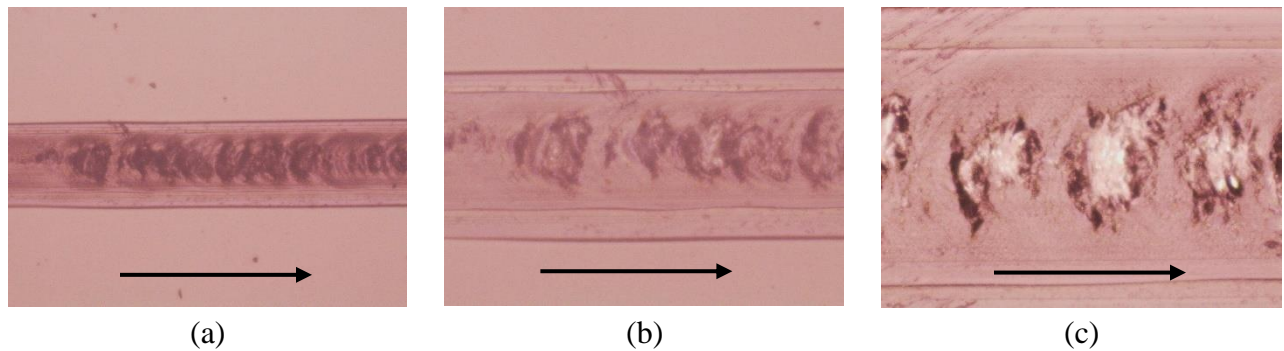


Figure 20. Onset of cracking in acrylic at 10 mm/s (a) 5X magnification; (b) 10X magnification; (c) 20X magnification. (Black arrow indicates the scratch direction)

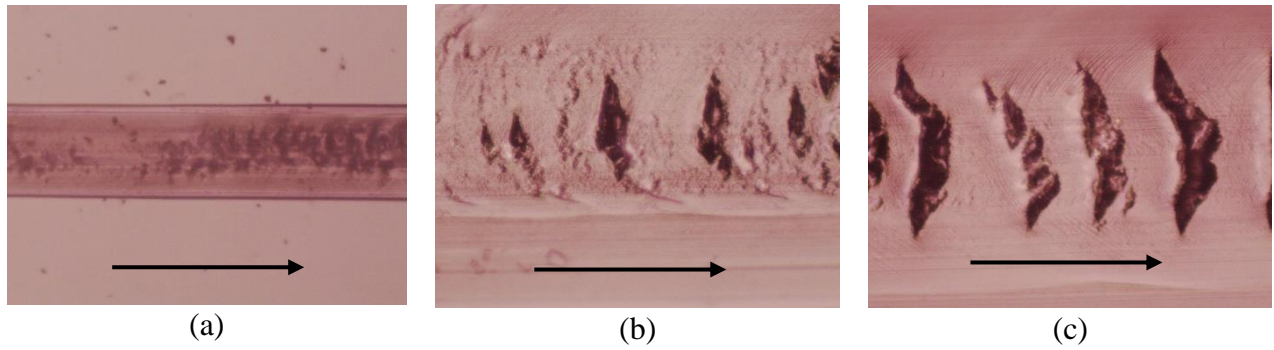


Figure 21. Onset of cracking in acrylic at 100 mm/s (a) 5X magnification; (b) 10X magnification; (c) 20X magnification. (Black arrow indicates the scratch direction)

Table 7. Onset load for cracking of acrylic at different scratch speed.

Scratch sample	Onset load for 1 mm/s	Onset load for 10 mm/s	Onset load for 100 mm/s
Scratch-1	44.47582766	39.98146605	26.64818376
Scratch-2	46.21078227	37.30571419	27.47835511
Scratch-3	46.18004752	39.86585125	23.96852292
Scratch-4	46.88875772	38.02030647	25.0998012
Average load	45.93885379	38.79333449	25.79871575
Standard Deviation	1.028734245	1.338224606	1.568531335

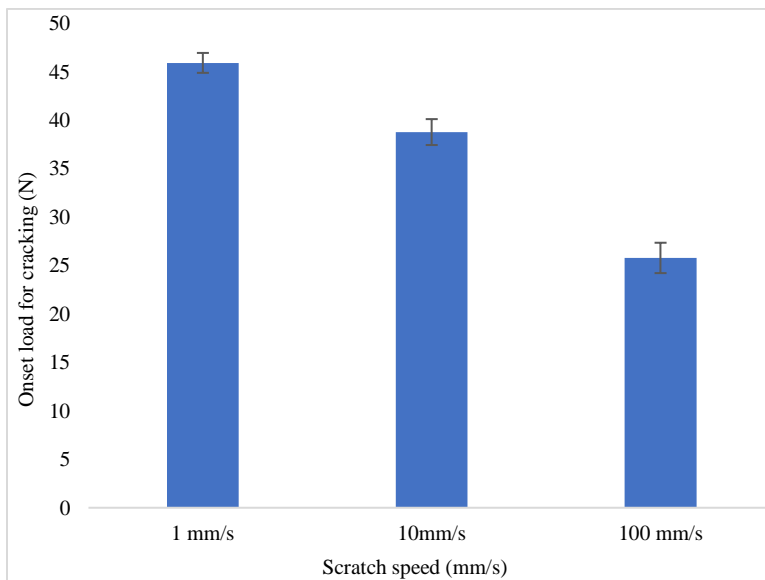


Figure 22. Onset load for cracking of acrylic at different scratch speeds.

For PC, change in scratch width along the scratch length was measured at 1 mm/s, 10 mm/s, and 100 mm/s, respectively. After the scratching process, the scratch widths along the scratch lengths of 20, 30, 40, 50, 60, 70, and 80 mm were measured. The gradual increase of scratch width along the scratch length is demonstrated in Figure 23, and the overall average reduction in scratch width with increase in scratch speed is shown in Tables 8-10. As shown in Figure 24, scratch width decreases with increase of scratch speed. The scratch width of PC decreases with increase in scratch speed because as the scratch speed increases PC tends to become stronger and stiffer (Figures 10-13), and hence the lower scratch width because of less plastic deformation with increase in speed. As such, the rate dependent mechanical behavior of PC can be related to the scratch behavior. During the tensile testing, as the crosshead speed increases the yield stress and the young's modulus of the PC increases, as shown in Figures 10 and 12. Similarly, as the scratch speed increases, PC shows smaller scratch width because of less plastic deformation with increase in speed.

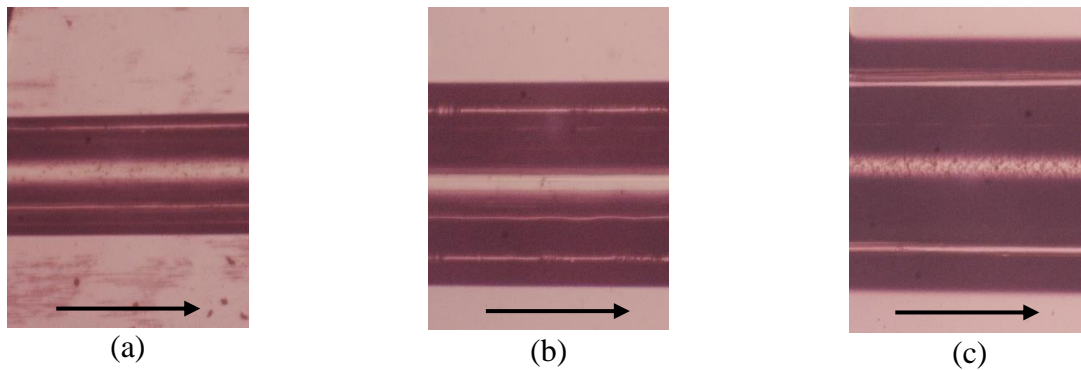


Figure 23. Images of scratch width along the scratch length for PC (a) Width at 20 mm; (b) Width at 50 mm; (c) Width at 80 mm. (Black arrow indicates the scratch direction).

Table 8. Scratch widths of PC for four different scratches at 1mm/s for different scratch lengths.

PC 1 mm/s	Sample-1	Sample-2	Sample-3	Sample-4	Average width
20 mm	0.4064	0.4230	0.4358	0.4474	0.4281
30 mm	0.5589	0.5525	0.5192	0.5358	0.5416
40 mm	0.6448	0.6282	0.6218	0.6128	0.6269
50 mm	0.7192	0.7576	0.7448	0.7526	0.7435
60 mm	0.7962	0.8358	0.8192	0.8282	0.8198
70 mm	0.8987	0.9179	0.9000	0.9192	0.9089
80 mm	0.9692	1.0115	0.9782	0.9820	0.9852

Table 9. Scratch widths of PC for four different scratches at 10 mm/s for different scratch lengths.

PC 10 mm/s	Sample-1	Sample-2	Sample-3	Sample-4	Average width
20 mm	0.4089	0.4205	0.4282	0.4217	0.4198
30 mm	0.4846	0.4833	0.5141	0.5064	0.4971
40 mm	0.5730	0.5666	0.6012	0.5974	0.5845
50 mm	0.6564	0.6602	0.6795	0.6770	0.6682
60 mm	0.7770	0.7538	0.7718	0.7718	0.7686
70 mm	0.8692	0.8628	0.8680	0.8718	0.8679
80 mm	0.9513	0.9474	0.9461	0.9590	0.9509

Table 10. Scratch widths of PC for four different scratches at 100 mm/s for different scratch lengths.

PC 100 mm/s	Sample-1	Sample-2	Sample-3	Sample-4	Average width
20 mm	0.3858	0.3897	0.3807	0.3782	0.3836
30 mm	0.4718	0.4782	0.4692	0.4741	0.4733
40 mm	0.5628	0.5705	0.5602	0.5500	0.5608
50 mm	0.6487	0.6525	0.6436	0.6590	0.6509
60 mm	0.7448	0.7487	0.7397	0.7384	0.7429
70 mm	0.8359	0.8346	0.8282	0.8397	0.8346
80 mm	0.9256	0.9243	0.9218	0.9295	0.9253

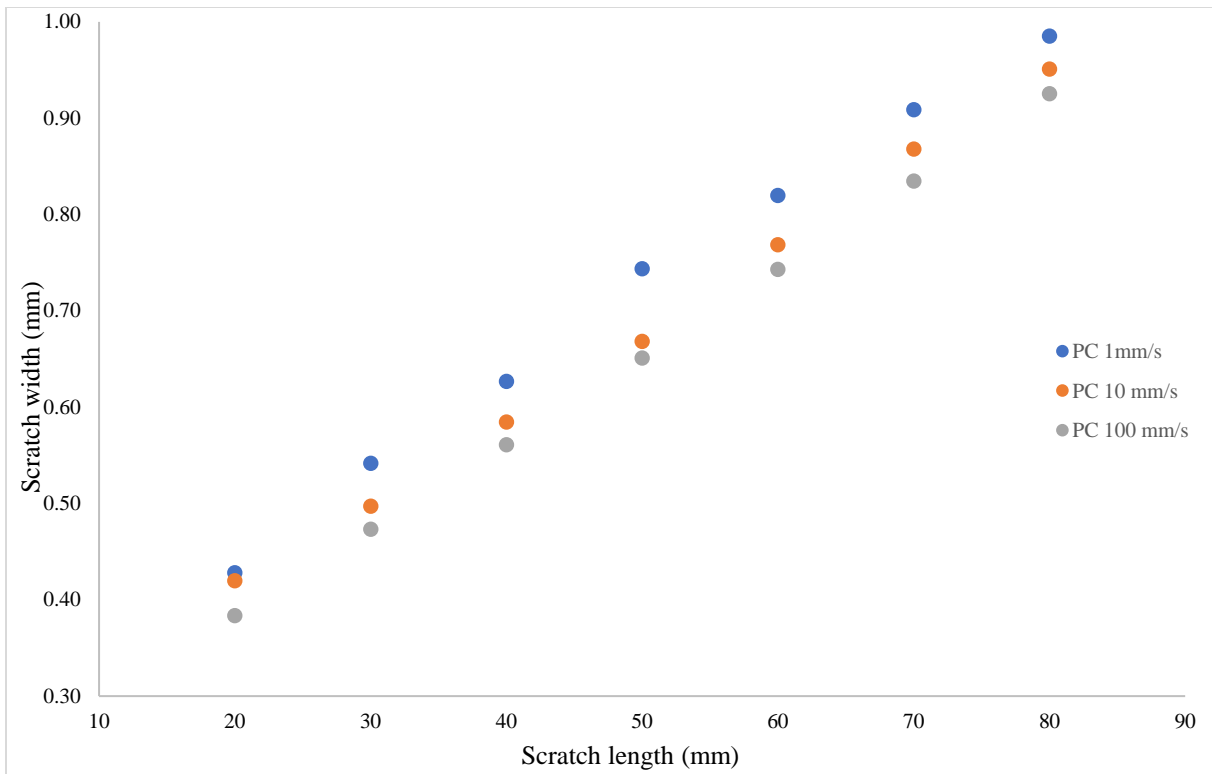


Figure 24. Scratch width as a function of scratch length for PC.

CHAPTER IV

FEM MODELING AND ANALYSIS

Finite Element Method (FEM) modeling is an effective tool for understanding the polymer behavior under various circumstances [16]. It is widely acknowledged that understanding the mechanical and scratch behavior of polymeric systems is crucial for their engineering applications. A commercial software, ABAQUS® [7] (V. 6.14) was used for the numerical analysis. The study focuses on the scratch behavior of polymers with varying material properties due to the increasing scratch normal load following the ASTM standard for scratch testing [17]. The dimensions of the model are 20x2x2 mm, as shown in Figure 25. As the scratching process is dynamic in nature, dynamic stress analysis was employed in the FEM simulation. Following the ASTM standard for scratch testing and due to symmetry condition, a half model is sufficient to model the entire structure [10]. The tip moves along the entire scratch length with a progressive load of 1-30 N.

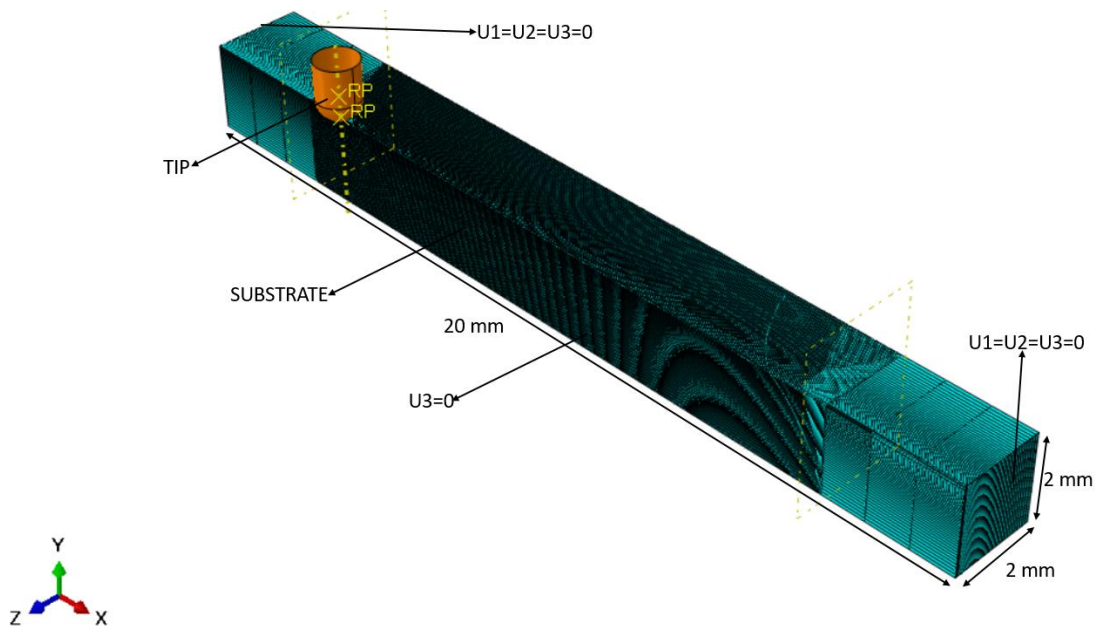


Figure 25. FEM model with a spherical tip of 1 mm diameter.

Nodes on both ends of polymer substrate were restricted to move in all directions and the bottom surface was restrained vertically to model the support for the specimen [18]. The scratch tip was considered to be rigid [2]. Eight Node 3D linear brick (C3D8R) element was used in the FEM simulation. The size of the element was 50 microns along the scratch length.

The FEM simulation of scratching process consists of three steps. The first step involves indenting the specimen with the scratch tip at a specified normal load. The second step involves the sliding of the indenter on the polymer surface at a specified scratch length and velocity with an increasing normal load. The tip is removed from the surface in the last step. Since a half model was used due to symmetry, the load applied on the scratch tip was half the actual value of applied load. To simulate crack formation during scratching, ductile damage criteria was used in the FEM model. According to the ductile damage criterion, the damage is initiated at point A and the damage evolution is the path A-B and B is the point of element removal, as shown in Figure 26 [19]. Damage initiation defines the point of initiation of degradation of stiffness. Elements can be removed from the mesh once the material stiffness is completely degraded [19].

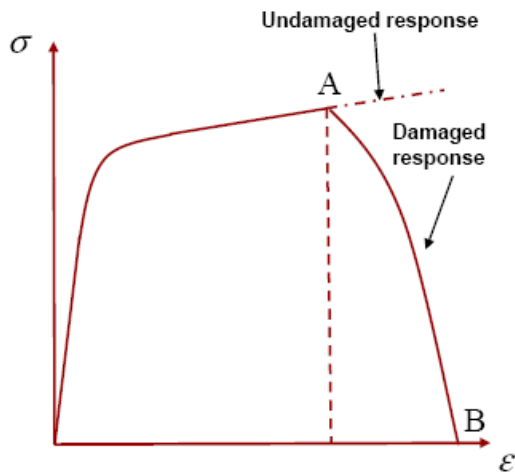


Figure 26. Typical material response showing progressive damage [19].

Ductile damage criterion was used in this study to analyze the effects of ductility, strength, coefficient of friction and stiffness on onset of cracking. When using ductile damage criterion, the behavior of crack is mainly influenced by stress triaxiality as a function of fracture strain [7]. The negative stress triaxiality indicates compressive stress and positive stress triaxiality indicates tensile stress scenarios [20]. Some assumptions were made (Table 11) such as when the stress triaxiality increases in tension, the fracture strain decreases, in-line with the literature [21]. Also, the damage does not initiate or propagate under compression. Therefore, high values of fracture strains were assumed in compression loadings.

Table 11. Triaxiality data used for the FEM modeling.

Fracture Strain	Stress Triaxiality
100	-10
100	-0.67
100	-0.33
50	0
1E-6	0.33
5E-7	0.67
1E-7	10

4.1 Effect of Ductility on Onset of Cracking

Material properties used for the FEM simulations to determine how the onset of cracking is changing with the change in ductility of the material is shown in Table 12. Three cases have been considered, with the first case the material has low ductility, in the second case material is moderately ductile and in the third case the material is brittle.

Table 12. Material properties used for FEM modeling to study the effect of ductility.

Young's modulus	3.5 GPa
Ultimate strength	60 MPa
Strain hardening slope	250 MPa
Coefficient of friction	0.6
Poisson's ratio	0.4
Density	1200 kg/m ³

The ductility of the material was varied by changing the fracture strain values for the triaxiality in the uniaxial direction. As the uniaxial fracture strain decreases the material tends to become more brittle. Here three different uniaxial fracture strain values were assumed: 0.01 for the moderately ductile material, 0.001 for the material with low ductility and 1E-6 for the brittle material. The corresponding biaxial and triaxial direction fracture strain values were assumed accordingly. Figure 27, shows the comparison of maximum principle stress contour for three different material types i.e. moderately ductile material, material with low ductility and brittle material. The white arrow shown in the Figures indicate the scratch direction. A ductile material tends to show better scratch resistance which can be seen in Figure 27(a), and as the ductility of the material decreases the scratch resistance tends to decrease, as shown in Figure 27(b), when all other material parameters are kept the same, the brittle material cracks shown in Figure 27(c), within the same load range. It can be concluded that, as the ductility of the material decreases the material is more prone to cracking during scratching. This can be compared with the experimental study where acrylic (brittle) cracked and the PC (ductile) did not show any cracks for a similar scratch normal load range. Also the scratch behavior changes with the change in scratch speed. As the scratch speed increases the material becomes more brittle and therefore cracks earlier i.e. the load for the onset of cracking decreases (Figure 22). It can be concluded

that the material with high ductility and low stiffness shows better scratch resistance in terms of cracking.

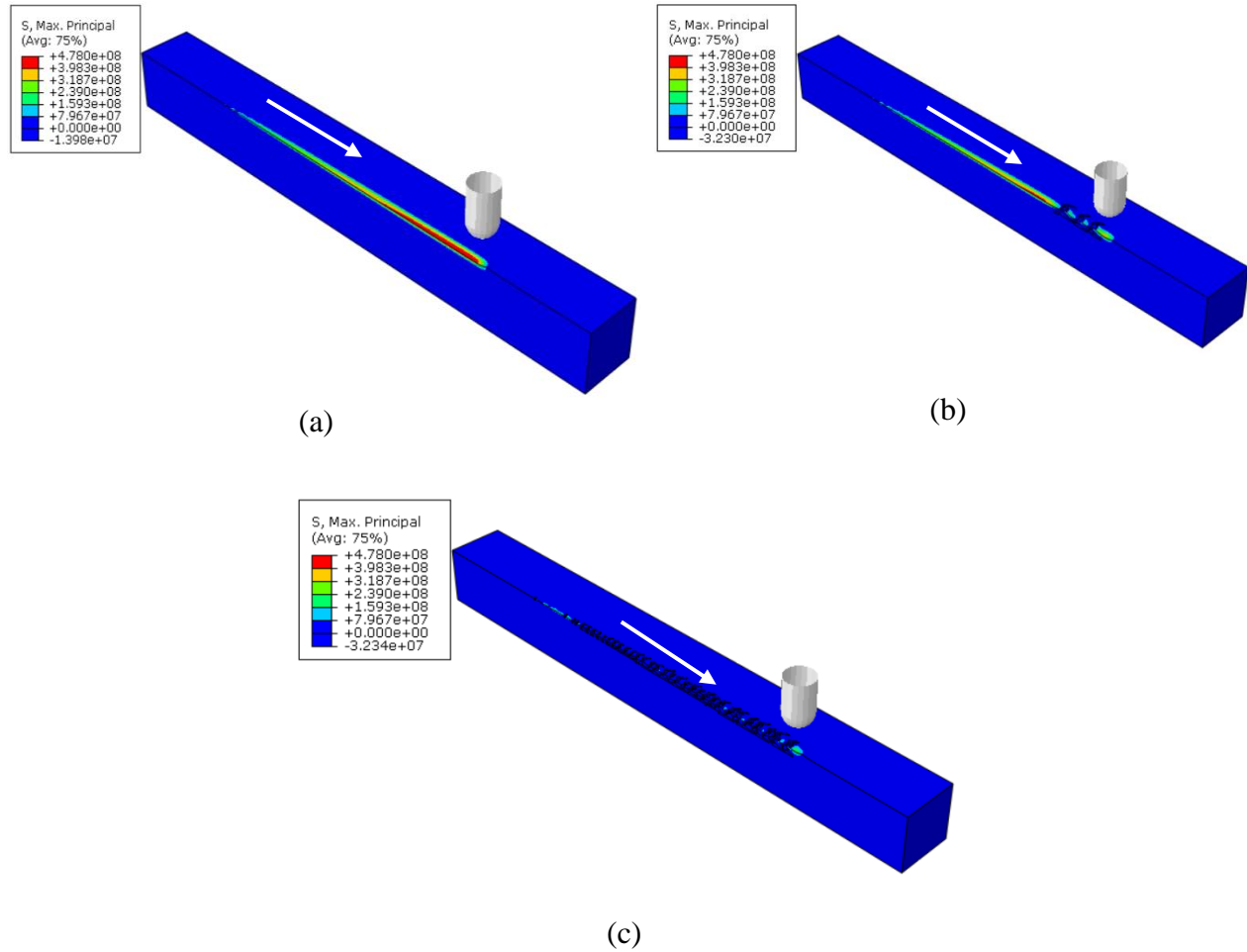


Figure 27. Maximum principle stress contour of materials with different ductility (a) Moderately ductile; (b) Low ductility; (c) Brittle. (White arrow indicates the scratch direction)

4.2 Effect of Strength on Onset of Cracking

The strength of the material plays a crucial role in scratch behavior of polymers. The three materials with different strengths of 60 MPa, 90MPa and 120 MPa were used in the FEM modeling. Here the strength of the material was varied to see how it affects the onset of cracking.

The material properties used for the FEM modeling are shown in Table 13. Figure 28, shows the comparison of maximum principle stress contour for three different material types. The white arrow indicates the scratch direction. As the strength of the material increases the distance for onset of cracking increases i.e. the material cracks much earlier for lower strength polymer, as shown in the Figure 28. It can be noticed that the onset of cracking for lower strength material is much earlier when compared to the onset of cracking for the higher strength material, it is evident that higher the strength of the material, higher the scratch resistance and its less prone to cracking. Browning et al. showed that as the strength of the polymer increases, the onset of cracking is delayed during scratching [22], similar to the FEM findings in this study. Thus, the experimental study conducted by Browning et al. [22] validates the FEM results in this study.

Table 13. Material properties used for FEM modeling to study the effect of strength.

Young's modulus	3.5 GPa
Ultimate strength	60 MPa, 90MPa, 120 MPa
Strain hardening slope	250 MPa
Coefficient of friction	0.6
Poisson's ratio	0.4
Density	1200 kg/m ³

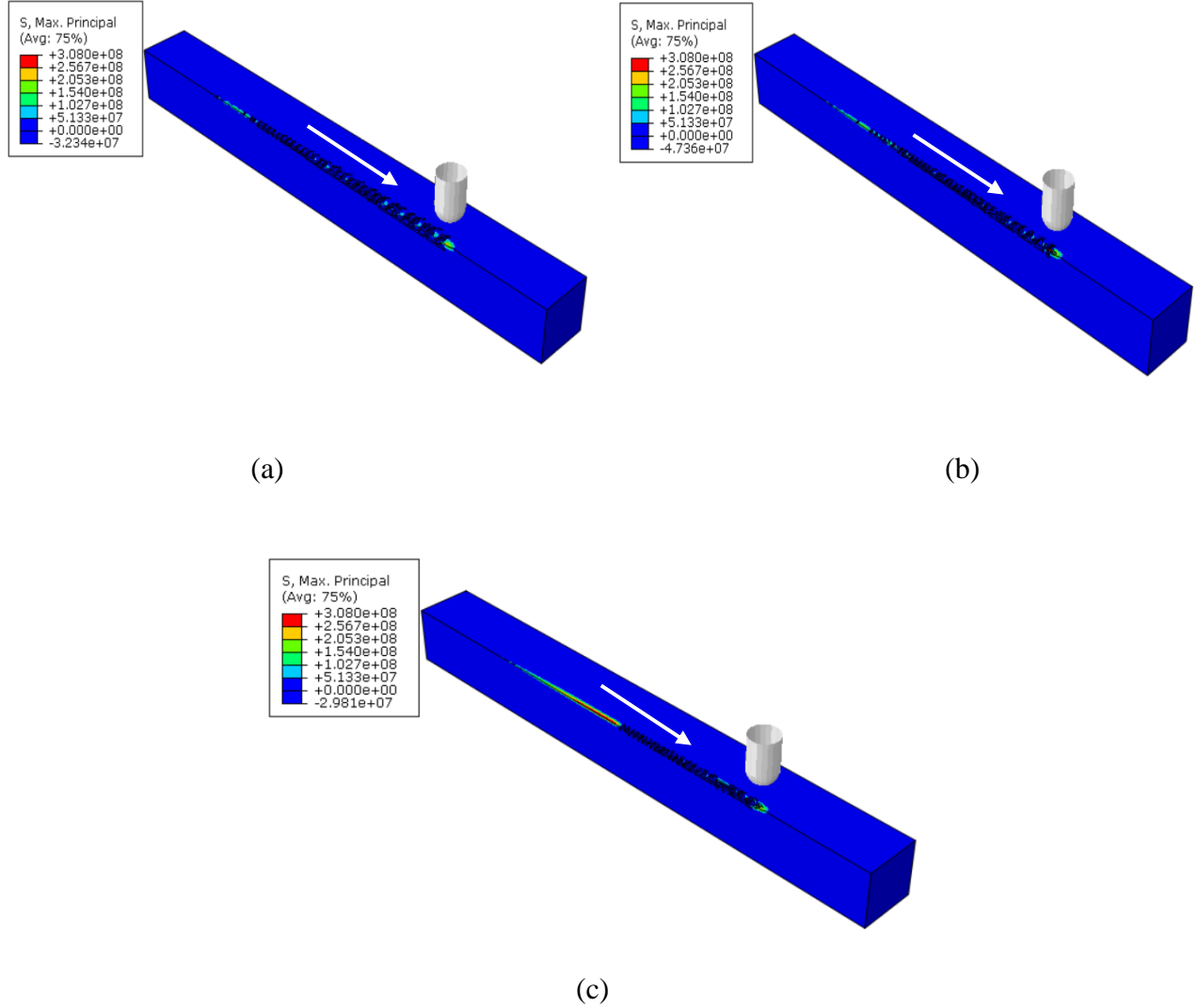


Figure 28. Maximum principle stress contour for materials with different strengths (a) 60 MPa; (b) 90 MPa; (c) 120 MPa. (White arrow indicates the scratch direction).

4.3 Effect of Coefficient of Friction on Onset of Cracking

Surface friction is a crucial factor during a scratching process. Surface friction greatly influences the stress field development during the scratching process [9]. The direction of the maximum principal stress is important in determining the type crack formation during scratching. In this study coefficient of friction (COF) was varied, i.e., COF of 0, 0.3, and 0.6 were used with all the other properties kept the same, to see how the onset of cracking is varying. The material

properties for the FEM analysis are shown in the Table 14. Figure 29, shows the maximum principle stress contour for materials with different COF. From Figure 29, it can be seen that the material with the highest COF shows cracking whereas the other two materials with a lower COF shows no cracking in the scratch path. Figures 30-31, show the maximum principle stress direction for models with different COF at scratch normal loads of 5.8 N and 25.1 N, respectively. The white arrow indicates the scratch direction. By the maximum principle stress direction, the type of cracking can be identified as tensile cracking, which can also be seen in the experimental study (Figure 19-21). It can be seen that for the same applied load, the model with COF 0.6 has the highest magnitude of principle stress at that point and hence cracks earlier. Also, the maximum principle stress is higher in the model with COF 0.3 when compared to the model with COF 0 at the same applied load. It can be said that the material with lower COF shows better scratch resistance with delay in onset of cracking. Thus, coefficient of friction can have a significant impact on onset of cracking.

Table 14. Material properties used for FEM modeling to study the effect of COF.

Young's modulus	3.5 GPa
Ultimate strength	60 MPa
Strain hardening slope	250 MPa
Coefficient of friction	0.0,0.3,0.6
Poisson's ratio	0.4
Density	1200 kg/m ³

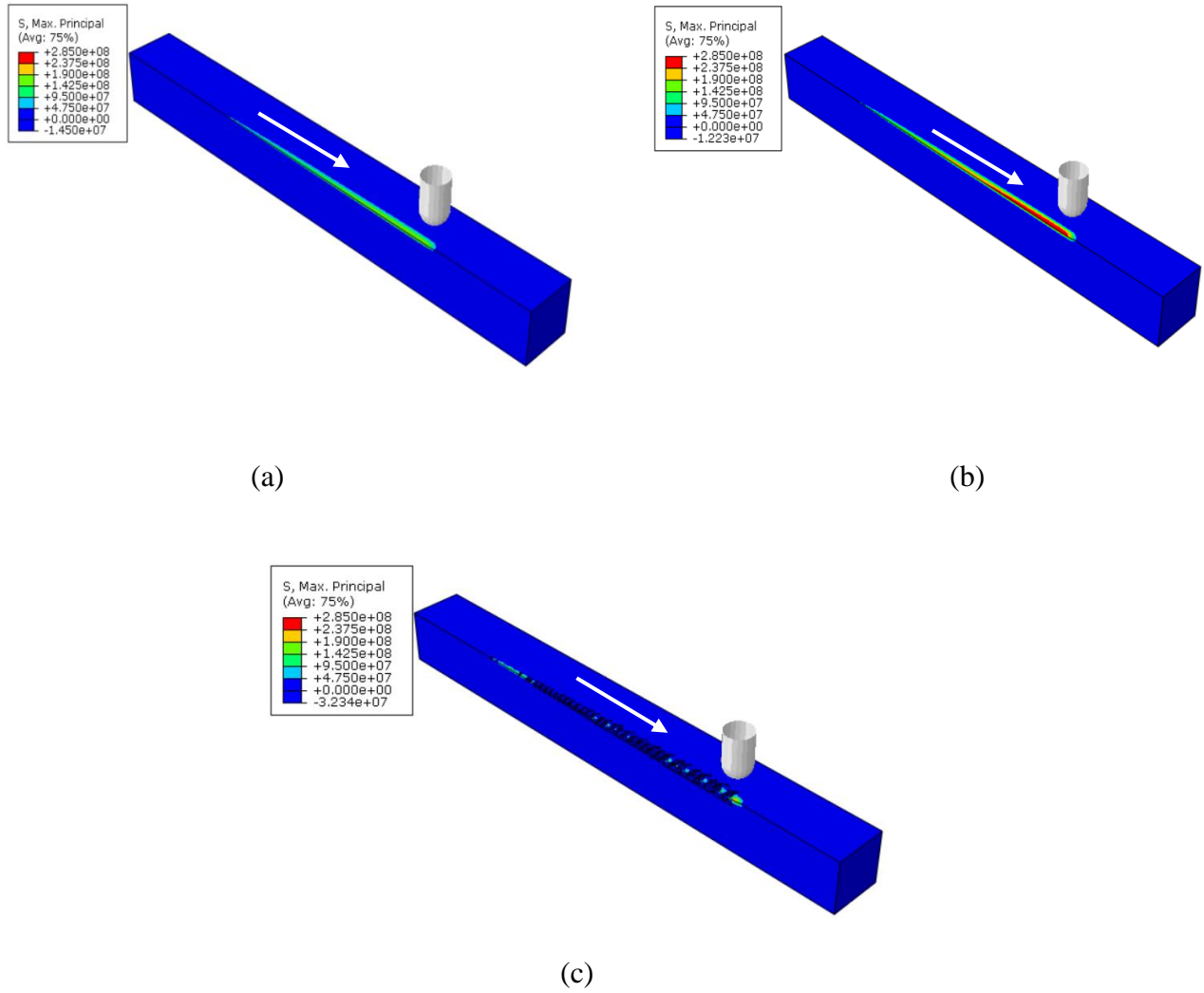


Figure 29. Maximum principle stress contour for FEM models with different coefficient of friction (COF) (a) COF: 0; (b) COF: 0.3; (c) COF: 0.6. (White arrow indicates the scratch direction).

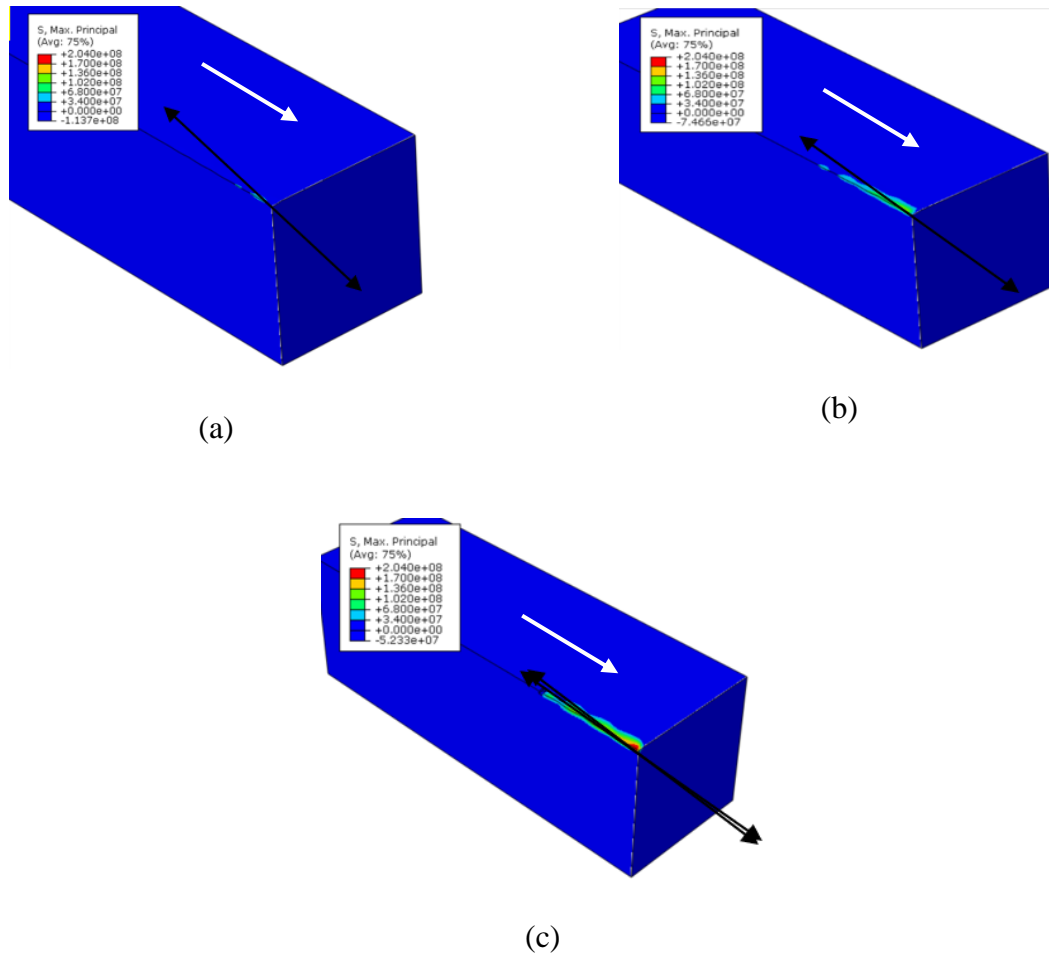


Figure 30. Maximum principle stress contour for FEM models at a load of 5.8 N (a) COF: 0; (b) COF: 0.3; (c) COF: 0.6. (Black arrow indicates the maximum principle stress direction)

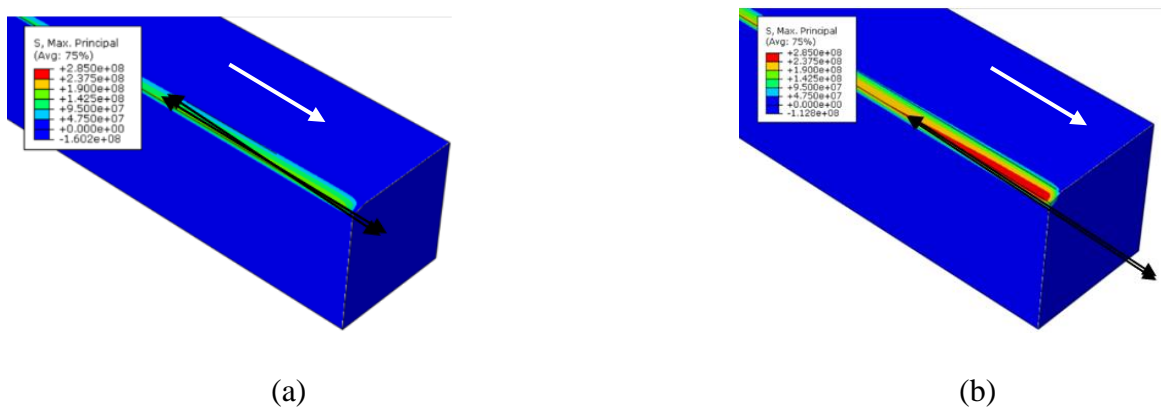


Figure 31. Maximum principle stress contour for FEM models at a load of 25.1 N (a) COF: 0; (b) COF: 0.3. (White arrow indicates the maximum principle stress direction)

4.4 Effect of Material Stiffness on Onset of Cracking

Now how the stiffness of the material affects the onset of cracking is discussed. The material properties used for the FEM simulations are shown in the Table 15. The three materials with different Young's modulus of 1.5 GPa, 2.5 GPa and 3.5 GPa were used. Figure 32, shows the maximum principle stress contour for FEM model with variation in Young's modulus. The white arrow indicates the scratch direction. From these simulations it can be seen that as the stiffness increases the scratch resistance decreases and the material is more susceptible for cracking which can be seen in Figure 32. From tensile testing for acrylic it was observed that as the crosshead speed increases the stiffness increases (Figure 16) also from the scratch testing it was observed that as the scratch speed increases the load for onset of crack decreases which is shown in Figure 22. It can be concluded that material with lower stiffness shows better scratch resistance in terms of crack formation.

Table 15. Material properties used for FEM modeling to study the effect of stiffness.

Young's modulus	1.5 GPa,2.5 GPa,3.5 GPa
Ultimate strength	60 MPa
Strain hardening slope	250 MPa
Coefficient of friction	0.6
Poisson's ratio	0.4
Density	1200 kg/m ³

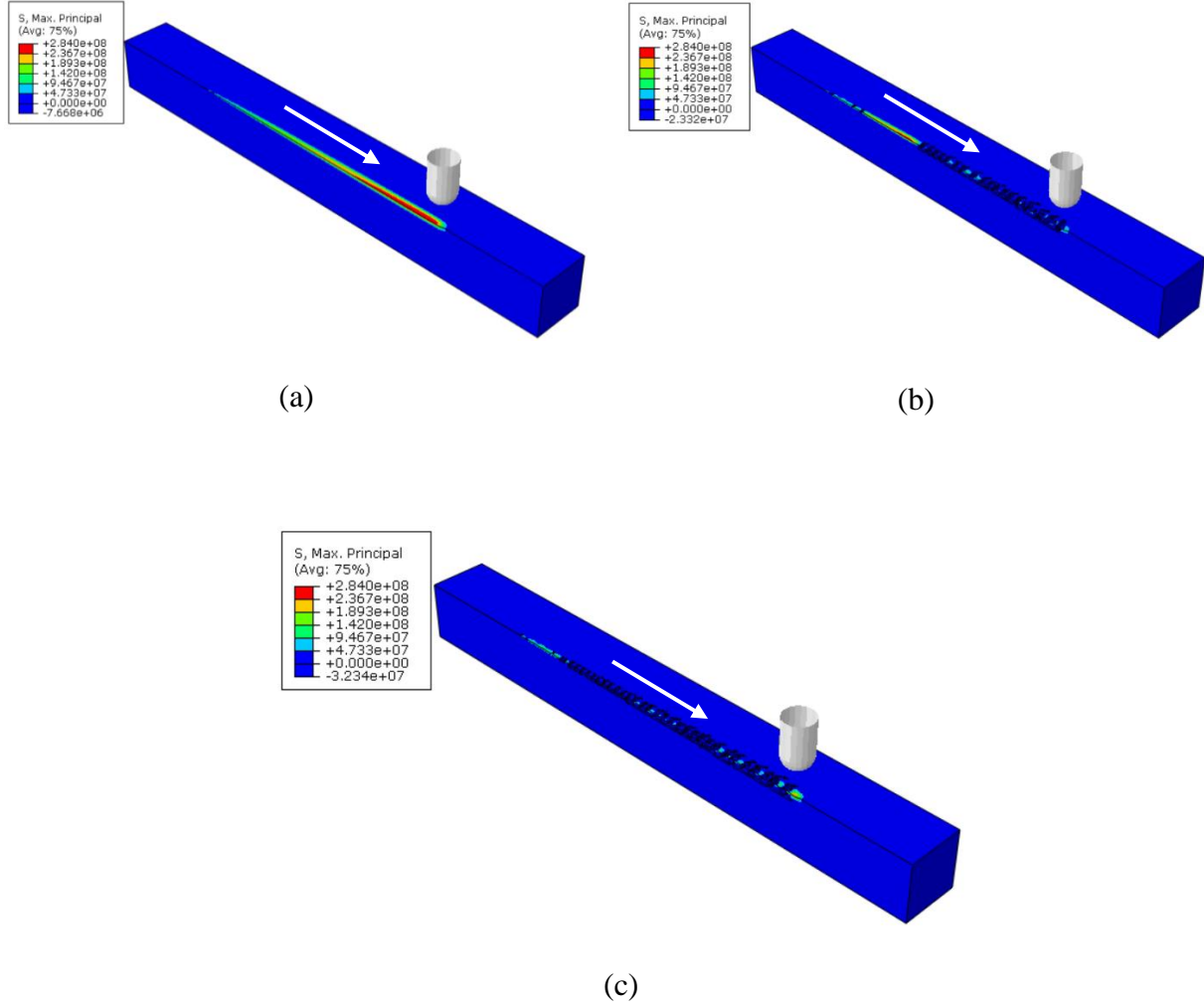


Figure 32. Maximum principle stress contour for FEM models with different Young's modulus (a) 1.5 GPa; (b) 2.5 GPa; (c) 3.5 GPa. (White arrow indicates the scratch direction).

CHAPTER V

CONCLUSIONS AND FUTURE SCOPE

5.1 Conclusions

The present research investigates how the scratch behavior of polymers is affected by the rate of testing, material properties and coefficient of friction. From the FEM simulations it was observed that some of the properties of the material an influence over the scratch behavior of polymers. These conclusions can be drawn from the FEM analysis and experimental work.

From the scratch testing it can be seen that for acrylic the onset of crack formation changes with change in scratch speed. As the scratch speed increases the length of the onset of crack decreases i.e. the material cracks at a lower load as scratch speed increases.

From the scratch testing it can also be seen that for PC there is no cracking observed but the width of the crack increases along the scratch length as the scratch speed decreases i.e. the width of the crack is smaller for a faster scratch speed.

From the tensile testing of PC and acrylic, it has been observed that both polymers became more brittle with increase in crosshead speed. The rate dependent mechanical behavior of the polymers explains the change in onset of cracking with change in scratching speed in acrylic, and change in scratch width with change in scratching speed in PC.

From the FEM simulations it can be seen that as the ductility of the material increases, the material is less prone to cracking when all the other material properties kept the same. The onset

of cracking is earlier for the brittle material, i.e., the material cracks at a much lower load. For ductile material, no cracking is observed.

From the FEM simulations it can be seen that as the strength of the material increases there is a delay in the onset of cracking when all other material properties kept the same, i.e., the material with lower strength cracks earlier and the material with higher strength cracks at a higher normal load.

As COF increases the surface of the material is prone to cracking, COF can have a significant impact on the onset of cracking. From the simulations it can be seen that as the COF increases the material cracks at a much lower load when all the other properties of the material are kept the same.

As the stiffness of the material increases the onset of cracking decreases, i.e. as the stiffness of the material increases the material cracks at a lower load.

In summary, changing certain material properties can significantly affect the onset of cracking, and, therefore, the scratch behavior of polymers. The FEM findings are also validated using experimental study on polymers.

5.2 Future Work

The current research can be extended to the following topics.

- I. Quantitative FEM analysis can be performed to better understand the scratch behavior of polymers. It can be achieved by doing an experimental analysis on mechanical properties of polymers such as tensile strength, strain softening slope, strain hardening slope, friction behavior of polymers, compressive behavior and post yielding behavior of polymers, and including these actual mechanical properties in the FEM model to perform quantitative analysis of polymer scratch behavior.
- II. Rate dependency, temperature dependency, pressure dependency and viscoelastic behavior can be considered to get an in-depth understanding of the scratch behavior. More realistic prediction of crack formation can be achieved by including these behaviors in the FEM model.
- III. Establish a set of criteria which can predict the crack formation during scratching for different polymers. If the scratch behavior can be predicted based on certain set of data using the FEM model that would be really helpful for product design.

REFERENCES

1. Friedrich, K., Sue, H. J., Liu, P., & Almajid, A. A. (2011). Scratch resistance of high-performance polymers. *Tribology International*, 44(9), 1032-1046.
2. Jiang, H., Browning, R., & Sue, H. J. (2009). Understanding of scratch-induced damage mechanisms in polymers. *polymer*, 50(16), 4056-4065.
3. Chivatanasontorn, V., Tsukise, S., & Kotaki, M. (2012). Surface texture effect on scratch behavior of injection molded plastics. *Polymer Engineering & Science*, 52(9), 1862-1867.
4. Lim, G. T. (2005). *Scratch behavior of polymers* (Doctoral dissertation, Texas A&M University).
5. Wong, M., Lim, G. T., Moyse, A., Reddy, J. N., & Sue, H. J. (2004). A new test methodology for evaluating scratch resistance of polymers. *Wear*, 256(11-12), 1214-1227.
6. Wong, M., Moyse, A., Lee, F., & Sue, H. J. (2004). Study of surface damage of polypropylene under progressive loading. *Journal of materials science*, 39(10), 3293-3308.
7. ABAQUS. ABAQUS® Analysis User's Manual, Version 6.9. Available from: www.simulia.com.
8. Baietto, M. C., Rannou, J., Gravouil, A., Pelletier, H., Gauthier, C., & Schirrer, R. (2011). 3D crack network analysis during a scratch test of a polymer: A combined experimental and multigrid X-FEM based numerical approach. *Tribology International*, 44(11), 1320-1328.
9. Hossain, M. M., Minkwitz, R., & Sue, H. J. (2013). Minimization of surface friction effect on scratch-induced deformation in polymers. *Polymer Engineering & Science*, 53(7), 1405-1413.
10. Hossain, M. M. (2013). *Quantitative modeling of polymer scratch behavior* (Doctoral dissertation, Texas A&M University).

11. Jiang, H., Lim, G. T., Reddy, J. N., Whitcomb, J. D., & Sue, H. J. (2007). Finite element method parametric study on scratch behavior of polymers. *Journal of Polymer Science Part B: Polymer Physics*, 45(12), 1435-1447.
12. Hossain, M. M., Jiang, H., & Sue, H. J. (2011). Effect of constitutive behavior on scratch visibility resistance of polymers—A finite element method parametric study. *Wear*, 270(11-12), 751-759.
13. Xiang, C., Sue, H. J., Chu, J., & Coleman, B. (2001). Scratch behavior and material property relationship in polymers. *Journal of Polymer Science Part B: Polymer Physics*, 39(1), 47-59.
14. Jiang, H. (2009). *Experimental and numerical study of polymer scratch behavior* (Doctoral dissertation, Texas A&M University).
15. ASTM International. (2014). *ASTM D638-14 Standard Test Method for Tensile Properties of Plastics*. Retrieved from <https://doi.org/10.1520/D0638-14>.
16. Reddy, J. N. (1993). *An introduction to the finite element method* (Vol. 2, No. 2.2). New York: McGraw-hill.
17. Hossain, M. M., Minkwitz, R., Charoensirisomboon, P., & Sue, H. J. (2014). Quantitative modeling of scratch-induced deformation in amorphous polymers. *Polymer*, 55(23), 6152-6166.
18. Hossain, M. M., Browning, R., Minkwitz, R., & Sue, H. J. (2012). Effect of asymmetric constitutive behavior on scratch-induced deformation of polymers. *Tribology Letters*, 47(1), 113-122.
19. Barany, T., Cziganya, T., & Karger-Kocsis, J. (2003). Essential work of fracture concept in polymers. *Periodica Polytechnica Mechanical Engineering*, 47(2), 91-102.

20. Hancock, J. W., & Mackenzie, A. C. (1976). On the mechanisms of ductile failure in high-strength steels subjected to multi-axial stress-states. *Journal of the Mechanics and Physics of Solids*, 24(2-3), 147-160.
21. Hadal, R. S., & Misra, R. D. K. (2005). Scratch deformation behavior of thermoplastic materials with significant differences in ductility. *Materials Science and Engineering: A*, 398(1-2), 252-261.
22. Browning, R., Sue, H. J., Minkwitz, R., & Charoensirisomboon, P. (2011). Effects of acrylonitrile content and molecular weight on the scratch behavior of styrene-acrylonitrile random copolymers. *Polymer Engineering & Science*, 51(11), 2282-2294.

VITA

Nikhil Reddy Aenugu was born in Telangana State, India. He received his Bachelor of Engineering Degree in Mechanical from Manipal University May 2015. In August 2016, Nikhil Reddy Aenugu began pursuing his Master's Degree in Mechanical Engineering at Texas A&M University-Kingsville and is expected to receive his M.S. in Mechanical Engineering Degree in December 2018.